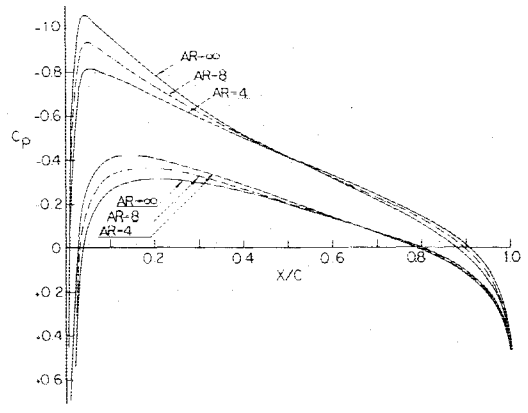

Fig. 1 Pressure distribution: elliptic wing, NACA-0012 cross section, $M_\infty = 0.63$, $\alpha = 2$ deg.

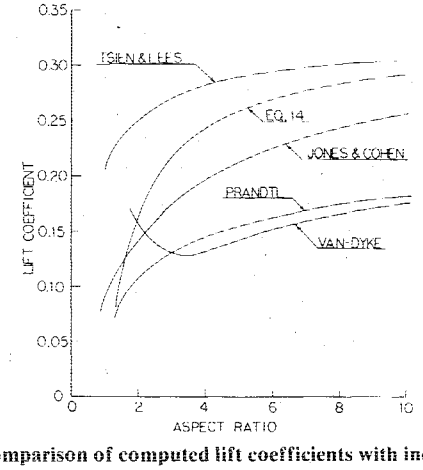

Fig. 2 Comparison of computed lift coefficients with incompressible lift coefficients corrected for compressibility effects.

for the elliptic NACA-0012 wing is shown in Fig. 1 for several different aspect ratio wings. The pressure distribution for the infinite wing showed excellent agreement with a solution[7] to the full inviscid equations. The lift coefficient as calculated from Eq. (10b) reduces to

$$C_L = \frac{\delta^{2/3}}{M_\infty^{3/4}}\left[\Gamma_0(0) + \frac{1}{\delta^{1/3}}\frac{4}{\pi}\frac{1}{\mathcal{A}}\Gamma_1(0)\right] \tag{14a}$$

$$C_L = 0.324 - 0.314/\mathcal{A} \tag{14b}$$

The first term represents the lift coefficient for a two-dimensional wing and the second term the correction due to finite aspect ratio. It should be noted that these results are derived from an asymptotic theory and are therefore formally valid as $\mathcal{A} \to \infty$. For an aspect ratio of 8 the lift of the finite wing is 13.7% less than the infinite aspect ratio wing.

While wind-tunnel test results are not available for comparison with these results, it is interesting to compare the computed lift coefficients to those calculated from incompressible lifting line theory corrected for compressibility effects. One method for correcting Prandtl's incompressible theory is based on a simple stretching of the wing chord by $1/\beta$. The corrected lift coefficient[8] is

$$C_L = 2\pi\alpha\mathcal{A}/(\beta\mathcal{A}+2) \tag{15}$$

A different correction

$$C_L = 2\pi\alpha\mathcal{A}/[\beta\mathcal{A}+2(1-\beta)] \tag{16}$$

in which the effective angle of attack is also modified has been proposed by Tsien and Lees.[9] Both these corrections are based on a stretching of the chord by $1/\beta$ and ignore thickness effects. The lift coefficients at infinite $\mathcal{A}$ disagree with the two-dimensional calculation. Multiplication of Eqs. (15) and (16) by $0.324/2\pi\alpha/\beta$ provides the correct asymptotic limit. The revised corrections and the computed result [Eq. (14)] are shown in Fig. 2. For comparison, results from Prandtl's and Van Dyke's[10] incompressible theories are shown.

V. Summary

The algorithm described is appropriate for computation of shock-free transonic flows about unswept wings. In addition to the subcritical flow calculated, supercritical flows can also be computed providing they are shock-free flows. The airfoil sections designed by Garabedian and Korn[11] and at NLR[12] fit this class. At present, the computer code is being modified to calculate flows with embedded shock waves.

Acknowledgment

This research was carried out with support of NASA Grant NSG 2171, Ames Research Center.

References

[1] Cook, L. P. and Cole, J. D., "Lifting Line Theory for Transonic Flow," *SIAM Journal of Applied Mathematics*, 1978, (in press).

[2] Murman, E. M. and Cole, J. D., "Calculation of Plane Steady Transonic Flows," *AIAA Journal*, Vol. 9, Jan. 1971, pp. 114-121.

[3] Krupp, J. A., "The Numerical Calculation of Plane Steady Transonic Flows past Thin Lifting Airfoils," Ph.D. Thesis, Univ. of Washington, Seattle, Wash., June 1971; also Boeing Scientific Research Labs, Rept. D180-1295B-1, June 1971.

[4] Small, R. D., "Numerical Solutions for Transonic Flow; Part 1—Plane Steady Flow over Lifting Airfoils," Dept. of Aeronautical Engineering, Technion, Haifa, Israel, TAE Rept. 273, Feb. 1976.

[5] Murman, E. M., "Analysis of Embedded Shock Waves Calculated by Relaxation Methods," *AIAA Journal*, Vol. 12, May 1974, pp. 626-633.

[6] Small, R. D., "Numerical Solutions for Transonic Flow Part 2: Transonic Lifting Line Theory," Dept. of Aeronautical Engineering, Technion, Haifa, Israel, TAE Rept. 294, April 1977.

[7] Lock, R. C., "Test Cases for Numerical Methods in Two-Dimensional Transonic Flows," AGARD, Rept. 575, 1970.

[8] Jones, R. T. and Cohen, D., *High Speed Wing Theory*, Princeton Aeronautical Paperbacks, Princeton University Press, 1960.

[9] Tsien, H. T. and Lees, L., "The Glauert-Prandtl Approximation for Subsonic Flows of a Compressible Fluid," *Journal of the Aeronautical Sciences*, Vol. 12, April 1945, pp. 173-187, 202.

[10] Van Dyke, M., "Lifting Line Theory as a Singular-Perturbation Problem," Dept. of Aeronautics and Astronautics, Stanford University, Stanford, Calif., SUDAER No. 165, Aug. 1963.

[11] Bauer, F., Garabedian, P., Korn, D., and Jameson, A., *Supercritical Wing Sections II*, Springer-Verlag, New York, 1975.

[12] Boerstock, J. W. and Huizing, G. H., "An Introductory Description of a Hodograph Method for Transonic Shock-Free Aerofoil Design," National Aerospace Laboratory, NLR, The Netherlands, NLR TR 73152 U, Nov. 1973.

Pressure Pulsations on a Flat Plate Normal to an Underexpanded Supersonic Jet

Lloyd H. Back* and Virendra Sarohia†
Jet Propulsion Laboratory, Pasadena, Calif.

Introduction

THIS Note is concerned with the interaction between an underexpanded supersonic gas jet and a flat plate with the

Received Oct. 25, 1977; revision received Jan. 26, 1978. Copyright © American Institute of Aeronautics and Astronautics, Inc., 1978. All rights reserved.

Index categories: Jets, Wakes, and Viscid-Inviscid Flow Interactions; Shock Waves and Detonations; Nonsteady Aerodynamics.

*Member, Technical Staff. Associate Fellow AIAA.
†Senior Scientist. Member AIAA.

plate located in a region in which the interaction produces shock wave and flow fluctuations.[1] In this study, the magnitude and frequency of pressure pulsations on the plate were determined so that fluctuating normal stresses exerted on solid structures can be evaluated.

System and Measurements

In the experimental investigation, nitrogen gas at ambient stagnation temperature flowed through a convergent nozzle with exit diameter $d = 2.03$ cm and impinged on a square metal plate normal to the jet (see insert, Fig. 1). The stagnation pressure P_0 of the jet was varied up to 8 atm. The dimension (15.2 cm square) of the plate was much larger than the nozzle exit diameter, unlike the system studied by Morch[2] at a particular nozzle pressure ratio. The distance s between the nozzle exit and the plate was 1.0 and 1.5 of the nozzle exit diameter. A fast-response pressure transducer with resolution of 0.00136 atm, rise time of 2 μs, and frequency response from 2 to 40,000 Hz was mounted flush on the plate at the jet centerline. Spark shadowgraphs also were taken of the flow and shock structure in the gap between the nozzle and plate.

Results

The results of this investigation are shown in Figs. 1-5. In Fig. 1, the magnitude of the peak-to-peak pressure fluctuation ΔP normalized by the ambient pressure P_∞ is shown as a function of the nozzle pressure ratio $R = P_0/P_\infty$ with spacing $s/d = 1.5$. For the range of nozzle pressure ratios investigated, there were two local peaks in ΔP, the first one at a pressure ratio of approximately 2 (near the choked flow condition of $R \simeq 1.9$) and the second peak at a pressure ratio of about 4.5. The corresponding values of $\Delta P/P_\infty$ were about 1 and 3, respectively. A study of the jet flow spark shadowgraphs and endwall pressure traces indicated that the first peak in pressure fluctuations ΔP at the plate occurred when the first shock cell and the oscillating shock wave present in front of the plate merged randomly to form a single oscillating shock wave. As the pressure was increased beyond $R \simeq 3.0$, only one shock cell was present in the jet flow. As the nozzle pressure ratio was increased to 4.33, this shock wave began to oscillate with large amplitude. (The maximum displacement of the shock wave was approximately 10% of the nozzle exit diameter.) This resulted in strong plate pressure fluctuations ΔP, as shown in Fig. 1. With such large pressure oscillations, it was possible to recover almost instantaneously on the plate the stagnation pressure upstream in the nozzle; i.e., at a nozzle stagnation pressure ratio of 4.6, the peak pressure ratio

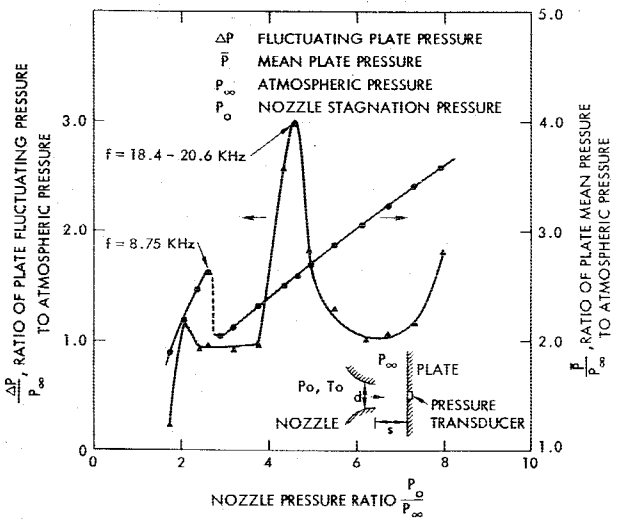

Fig. 1 Variation of plate mean and fluctuating pressures with nozzle pressure ratio; spacing $s/d = 1.5$.

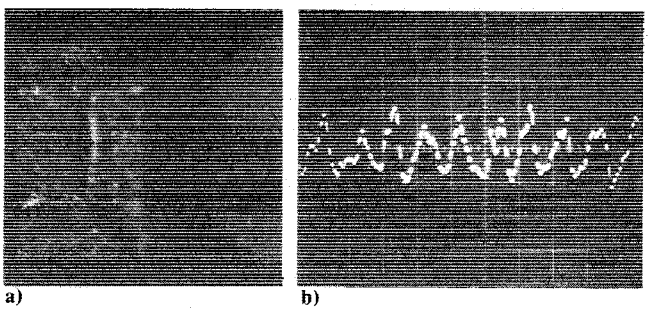

Fig. 2 a) Shadowgraph of jet flow between nozzle exit and plate; and b) plate fluctuating pressure trace with vertical scale 13.16 psi/division, horizontal scale 50 μs/division. Nozzle pressure ratio $R = 4.33$; spacing $s/d = 1.5$.

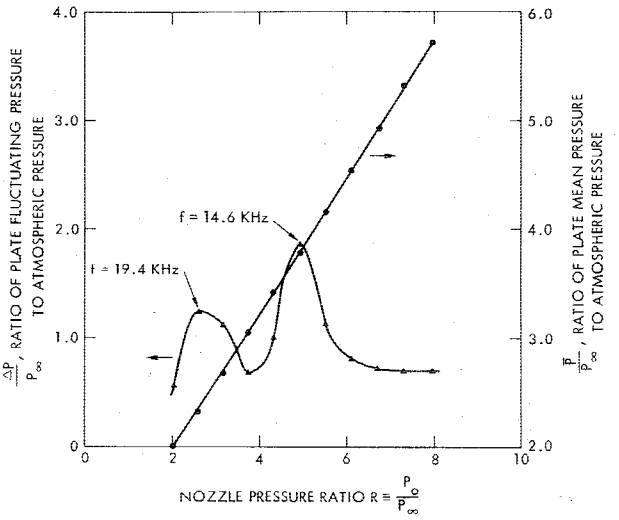

Fig. 3 Variation of plate mean and fluctuating pressure with nozzle pressure ratio; spacing $s/d = 1.0$.

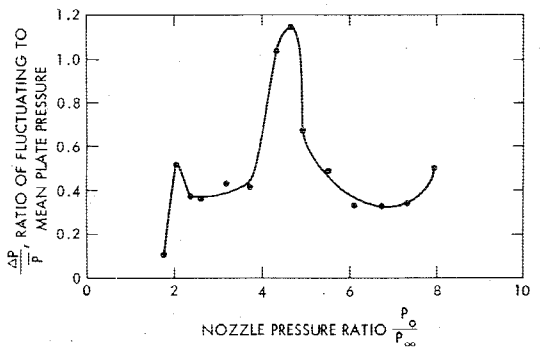

Fig. 4 Ratio of plate fluctuating to mean pressure for different nozzle pressure ratio; spacing $s/d = 1.5$.

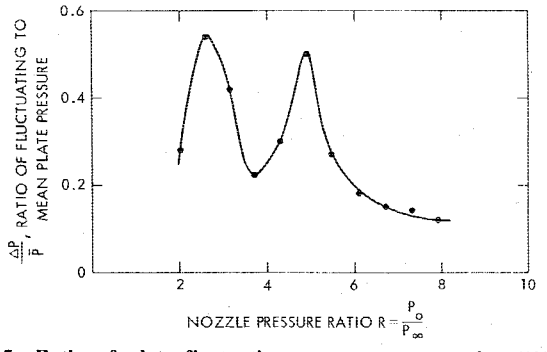

Fig. 5 Ratio of plate fluctuating to mean pressure for different nozzle pressure ratio; spacing $s/d = 1.0$.

on the plate $(\bar{P}/P_\infty) + \frac{1}{2}(\Delta P/P_\infty) = 4.1$. The strength of these pressure pulsations then decreased as the nozzle pressure ratio R was increased. Figure 2 indicates the fluctuating pressure trace and one of the shadowgraphs at a pressure ratio of 4.33 when large-amplitude shock oscillations occurred. The normal shock wave standing in the jet flow oscillated at a frequency f of about 20 kHz. (Frequencies at the pressure peaks are indicated in Figs. 1 and 3.)

Placement of the plate in the vicinity of the first shock cell of the corresponding freejet (without the plate) produced a spatial zone of shock-wave instability therein and caused the shock wave to oscillate, which resulted in periodic pressure pulsations on the plate. At a lower pressure ratio of about 2.5, the pressure fluctuations ΔP were less because of the interaction of relatively weak diamond shock in the jet. As the nozzle stagnation pressure ratio R was increased, the mean pressure $\bar{P}$ on plate increased (Fig. 1). At higher stagnation pressures, larger pressure losses occurred across the shock waves; i.e., the increase in plate recovery pressure is not directly proportional to the increase in jet stagnation pressure. The local peak and the decrease in mean plate pressure at a nozzle pressure ratio of about 2.6 (Fig. 1) was associated with the weaker diamond shocks in the jet changing to a stronger normal shock cell (Mach disk) as the pressure ratio was increased.

The ratio of the pressure fluctuation ΔP to the mean pressure $\bar{P}$ on the plate, i.e., what the plate experiences, is shown in Fig. 4 with spacing $s/d = 1.5$. The magnitudes of the pressure fluctuations with respect to the mean pressure were relatively large; at the first peak, $\Delta P/\bar{P}$ was about 0.5, and at the second peak, $\Delta P/\bar{P}$ was more than 1.0.

Pressure data obtained with a smaller plate spacing of $s/d = 1.0$ are shown in Figs. 3 and 5. For the first peak, the pressure fluctuations were about the same as for the larger spacing, but for the second peak the pressure fluctuations were less by 0.5 (cf. Figs. 4 and 5). This was due to the smaller amplitude of the standing shock-wave oscillations and less pressure loss across the shock (higher $\bar{P}$) for the smaller spacing.

Conclusions

The experimental investigation revealed local peak pressure fluctuations on the plate at nozzle pressure ratios of approximately 2 and 4.5, with the latter case producing fluctuations of the same order as the mean pressure on the plate. The frequency of the oscillations was as large as 20 kHz. For choked jet flow at ambient pressure higher than atmospheric, the pressure fluctuations would increase accordingly, and, therefore, adjacent solid structures would be subjected to proportionately higher normal stresses. The shock-wave oscillations in the axially varying velocity field of the jet produce stagnation pressure changes across the shock and corresponding pressure pulsations on the plate.

Acknowledgment

This work presents the results of one phase of research carried out in the Energy and Materials Research Section of the Jet Propulsion Laboratory, California Institute of Technology, under contract NAS 7-100, sponsored by NASA.

References

[1] Semiletenko, B. G. and Uskov, V. N., "Empirical Formulas for Locating Shock Waves in a Jet Impinging on a Barrier at Right Angles," *Inzhenerno-Fizicheskii Zhurnal*, Vol. 23, Sept. 1972, pp. 453-458 (English transl., Consultant's Bureau, New York).

[2] Morch, K. A., "A Theory for the Mode of Operation of the Hartmann Air Jet Generator," *Journal of Fluid Mechanics*, Vol. 20, Pt. 1, Sept. 1964, pp. 141-159.

Round Jet in a Cross Flow: Influence of Injection Angle on Vortex Properties

Dolores Krausche* and Richard L. Fearn†
University of Florida, Gainesville, Fla.
and
Robert P. Weston‡
NASA Langley Research Center, Hampton, Va.

Introduction

THE study of a turbulent jet of fluid injected at a large angle into a cross flow is motivated by several applications of interest, including the cooling of combustion products and the aerodynamics of V/STOL aircraft. One configuration that has been studied extensively is that of a round subsonic jet of air discharging through a large flat plate into a uniform subsonic cross flow. A dominant and persistent feature of this flow is a pair of diffuse contrarotating vortices that are deflected by the cross flow and swept downstream. A model developed by Fearn and Weston has been utilized to infer the properties of the vortex pair from selected velocity measurements for perpendicular jet injection into the cross flow.[1] These vortices play an important role in determining the pressure distribution on the surface through which the jet exhausts, and it is this pressure distribution that is of primary importance in V/STOL aerodynamics. The purpose of this Note is to present the effects of jet injection angle on the properties of the vortex pair associated with a jet in a cross flow.

Experiment

The experiment was conducted in the V/STOL wind tunnel at NASA Langley Research Center, Hampton, Va. The apparatus utilized in previous tests [1,2] was modified to provide for jet injection angles δ of 45, 60, 75, 90, and 105 deg into the cross flow. A round jet of air 10.16 cm (4.00 in.) in diameter was discharged through a horizontal flat plate into the cross flow of the wind-tunnel test section. Effective jet-to-cross flow velocity ratios of 4 and 8 were studied. As in previous tests, velocities were determined with a rake of seven yaw-pitch probes.

Results

A description of the diffuse vortex model and the procedure for inferring the properties of the contrarotating vortex pair associated with a jet in a cross flow from velocity measurements are provided in Ref. 1. The physical properties of the vortex pair for the cases studied in this experiment are presented in Figs. 1-3. Each point on a graph represents a value of a parameter inferred from velocity measurements in a given cross section of the jet plume. In each of these graphs, a vortex property is plotted vs arc length S along the vortex curve (the curve defined by projecting the vortex trajectories onto the plane of flow symmetry). All lengths are nondimensionalized by the jet diameter D, and the effective vortex strength is nondimensionalized by the factor $2DU_\infty$,

Received Dec. 21, 1977; revision received Feb. 10, 1978. Copyright © American Institute of Aeronautics and Astronautics, Inc., 1978. All rights reserved.

Index categories: Aerodynamics; Boundary Layers and Convective Heat Transfer—Turbulent; Jets, Wakes, and Viscid-Inviscid Flow Interactions.

*Postdoctoral Associate, Department of Engineering Sciences.
†Associate Professor, Department of Engineering Sciences. Member AIAA.
‡Associate Engineer, Low Speed Aerodynamics Branch.